The Investigation of Land Surface Retrieval Methods Using Landsat 5 and 8 Data for Urban Heat Island Effect in Mandalay Area

Khin Mar Yee[1], Mu Mu Than[2], Kyi Lint[3], Moe Thidar Htwe[4], Mar Lar Han[5], Kyi Khaing[6]

Abstract

In this paper the urban heat islands (UHI) effect in Mandalay City has been identified by retrieving the land surface temperature (LST) distribution. The aim of this paper is to implement an algorithm to measure land surface temperature of Mandalay city. The Land surface temperature has been estimated by using Single Channel (SC) algorithm. These two algorithms can be implemented using Landsat 5 and Landsat 8 satellite data. The various methods adopted for retrieving the algorithm has been addressed in the present study. Moreover, the intension of this study is to analyze with demonstration and verify the spatial distribution property of the LST with urban spatial information, related Normalized Difference Vegetation Index (NDVI) using the Remote Sensing (RS) data and Geographic Information System (GIS). The presence of LST was analyzed using Landsat 5 Thematic Mapper (TM) and Landsat 8 Operational Land Imager (OLI) images. The final output it is revealed that barren lands, uncultivable land and urban areas experienced high LST and the areas with high vegetation cover and water body experiencing low LST. The results from both the algorithms show a variance of 4ºC between urban areas within one decade, barren lands and vegetation covers thus indicating the presence of UHI in Mandalay city.

Keywords: Landsat, Land Surface Temperature (LST), Single Channel (SC) algorithm, Thermal infrared (TIR), Normalized Difference Vegetation Index (NDVI)

Introduction

Urbanization is the main cause of urban transformation and they impact on Land Surface Temperature (LST). The rapid urban expansions have caused urban changes, which affect the ecological environmental process at local and regional levels, especially the Urban Heat Island (UHI) [1] [2] [3]. Urban changes are manifested through conversion and modification, which are caused by interactions between climatic and anthropogenic forces owing to its inherently complex nature [4] [5]. With increasing urbanization, understanding the impacts of climate change upon the urban environment will become ever more important. This increasing trend in global urbanization influenced many researchers to investigate the potential impacts of man-made activities on urban thermal environment such as LST and UHI effect [6]. Because of the urbanization, where the natural vegetation areas are replaced by impervious surfaces, such as metal, asphalt and concrete [7] [8].

Currently, urbanization is considered the most important driver of climate change [9]. Unplanned and haphazard urbanization coupled with the poor building design are the biggest causes of heat islands in cities. As addressed in previous studies, intensive and rapid urbanization changes, which has exacerbated the ongoing impacts on the climate system [10]). Lambin et al. (2003) further indicate that the complexity of these factors can be simplified to themes that relate various drivers to particular urban changes or primary cause of LST change.

[1] Associate Professor, Department of Geography, Dagon University
[2] Associate Professor, Department of Geography, Dagon University
[3] Professor and Head, Department of Geography, Dagon University
[4] Professor, Department of Anthropology, Yadanabon University
[5] Associate Professor, Department of Geography, Dagon University
[6] Assistant Lecturer, Department of Geography, Yadanabon University

This is because the importance to these factors depends on the situation and spatial scale of study. Research has shown that UHI is primarily caused by the built environment in urban areas, in which natural areas are replaced with non-permeable and high temperature surface of concrete and asphalt [11]. The distinct behaviors of the urban thermal environment are related to urbanization both in natural and anthropogenic surface [12] [3] as different surfaces modify the structure, composition, and energy balance of the environment. The investigation of research works related with urban growth, socio-economic situation for Mandalay City and analysis of urban sustainable development and transformation were examined [13] [14]. Despite the fact that Mandalay exert strong centripetal forces and were rapidly growing cities of Myanmar, there was a scarcity of research on urban changes and the creation of microclimates. Considering the importance of the observation of LST and NDVI changes, it was become an imperative area of this research. Therefore, this paper approached to investigation of the LST changes and analyzed on the regression of correlation between LST and NDVI. Mandalay is the second largest city in Myanmar. It is located on the eastern bank of the Ayeyarwady River. The population is 1, 335,553 (2014 census). Mandalay was founded in 1857 by King Mindon, replacing Amarapura as the new royal capital of Konbaung dynasty. It was Myanmar's final royal capital before the kingdom's annexation by the British Empire in 1885. Under the British rule, Mandalay remained commercially and culturally important despite the rise of Yangon, the new capital of British Burma. Today, Mandalay is the economic center of Upper Myanmar [15]. (Fig. 1).

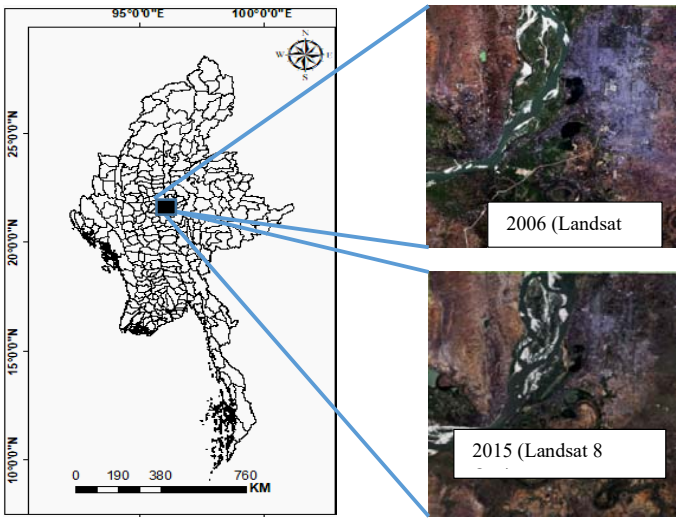

Figure (1). Study Area in Myanmar

Data and Methodology

For the research paper, satellite data needed to estimate LST and associated with the NDVI of Mandalay City. Since the objective was observed to changes of the thermal condition of Landsat 5 and Landsat 8 for Mandalay City. The images were taken ten year interval and represented the nearly the same date. To measure the quantitatively LST intensity and NDVI, the study areas were selected from Landsat 5 Thematic Mapper (TM) images and Landsat OLI 8 images of March, 2006 and 2015 for Mandalay City. Imageries of satellites were distributed free from the following United States of Geological Survey (USGS). Details of the remoted sensed data of this study were shown in Table 1 and 2.

Table (1). Acquisition of Landsat Satellite Images L5 TM 2006

Metadata Details of TM (Landsat 5)		
Sensor	Optical	Thermal
Date of Acquisition	2006– 03-05	
Sun Elevation	54.40392701	
Path/Row	133/45	
Cloud cover	1	
Band	6	1
Resolution	30 m	100 m
Radiance- Mult-Band-6	:	5.5375E-02
Radiance-Add-Band-6	:	1.18243
K_1 for Band 6	:	607.76
K_2 for Band 6	:	1260.56

Source: MLT data of Landsat 5, USGS

Table (2). Acquisition of Landsat Satellite Images L8 OLI 2015

Metadata Details of TIRS and OLI (Landsat 8)		
Sensor	Optical	Thermal
Date of Acquisition	2015– 03-14	
Sun Elevation	55.40720673	
Path/Row	133/45	
Cloud cover	1.97	
Band	9	2
Resolution	30 m	100 m
Radiance- Mult-Band-10	:	3.3420E-04
Radiance-Mult-Band-11	:	3.3420E-04
Radiance-Add-Band-10	:	0.10000
Radiance-Add-Band-11	:	0.10000
K_1 for Band 10	:	774.8853
K_1 for Band 11	:	480.8883
K_2 for Band 10	:	1321.0789
K_2 for Band 11	:	1201.1442

Source: MLT data of Landsat 8 OLI, USGS

Landsat 5 multispectral image and Landsat 8 multispectral image series were used as remote sensing data source for the study. Landsat satellite images (2006 and 2015) were downloaded from the official website of United States Geological Survey (USGS) and used in order to reach the research objectives. The data used in the study includes Landsat 5 data for 2006 (2006-03-05) and Landsat 8 (OLI) 2015 (2015-03-14) which were cloudless area. Spatial resolution is 30x30 m. UTM zone is 47 and Datum is WGS 84. The procedures of this paper consist of three phases.

The second phase is retrieval of the LST of 2006 and 2015. To operate the retrieve for the LST, the calculation of NDVI and Land Surface Emissivity (LSE) were necessary to apply to estimation of LST. The principal of NDVI is that the reflexes rates are differ at the Near Infrared (NIR) and RED band. This equation is denoted as the following formula. Healthy vegetation absorbs most of the visible light that hits it, and reflects a large portion of the near-infrared light. Sparse vegetation reflects more visible light and less near-infrared light. NDVI ranges from minus one (-1) to plus one (+1).

$$NDVI = (NIR-R) / (NIR+R)$$

ε is land surface emissivity, which was obtained using NDVI Threshold Methods. The formula of P_v is the vegetative proportion as following;

$$P_v = \{(NDVI - NDVI_{min}) / (NDVI_{max} - NDVI_{min})\}^2$$

Where P_v indicated the vegetation proportion, ε due to $\varepsilon_{veg} P_v + \varepsilon_{soil} (1- P_v)$, where ε_{veg} is vegetation emissivity, ε_{soil} means soil emissivity.

The most appropriate procedure to retrieve LST from a SC located in the TIR region. The main goal of the SC method is to obtain an algorithm to retrieve LST from one thermal band of the sensor. The processing for Calculation of LST, LST was retrieved from the

thermal infrared band (TIR) of Landsat TM 5. First, the Digital Numbers (DNs) of band 6 are converted to radiation luminance (R_{TM6}, m W cm^{-2} sr^{-1}) by the following formula,

$$R_{TM6} = \frac{V}{255} (R_{max} - R_{min}) + R_{min}$$

Where, R_{TM6} is the spectral radiance, V represents the Digital Number of band 6 received by the sensor, R_{max} is the minimum DN; R_{min} (Wm^{-2} $sr^{-1}\mu m^{-1}$) are the minimum and maximum detected spectral radiances, (R_{max} =1.896, R_{min} =0.1534 (mW^{*} $cm^{-2*}sr^{-1}$)).

Standard Landsat 8, the digital numbers of TIRS band data were transform OLI and TIRS band data was converted to Top of Atmosphere (TOA) spectral radiance using the radiance rescaling factors provided in the metadata file with the following equation;

$$L_\lambda = M_L Q_{cal} + AL$$

Where, L_λ means TOA spectral radiance and M_L is band specific multiplicity rescaling factor from the metadata, AL indicates for band specific additive rescaling factor from the metadata and Q_{cal} can be Quantized and calibrated standard product pixel values. Brightness temperature (T_b) is the microwave radiation radiance traveling upward from the top of Earth's atmosphere. The calibration process has been done for converting thermal DN values of thermal bands of TIR to T_b. For finding T_b of an area the TOA spectral radiance of (L_λ) was needed.

The second step, the radiation luminance of the all satellite images were converted to at-satellite brightness temperature in Kelvin, T (K), using the following formula for all Landsat images.

$$Tb = \frac{K_2}{\ln(\frac{K_1}{L_\lambda} + 1)}$$

Where, T_b defines the meaning of the effective at satellite brightness temperature in Kelvin (K), $\mathbf{L_\lambda}$ is TOA spectral radiance and K_1 and K_2 are the band specific thermal conversion constant from metadata (pre-launch calibration constants). The following Table 2.2 distinguished the respective value of band conversion constant from metadata.

Table (3). Band Specific Thermal Conversion Constant from metadata

Sensor	K_1 (watt/ (m^2 x ster x μm))	K_2 (watt/ (m^2 x ster x μm))
Landsat 5 TM	1260.56	607.76
Landsat 8 OLI	BAND_10 = 774.8853	BAND_10 = 1321.0789
	BAND_11 = 480.8883	BAND_11 = 1201.1442

Source: MLT data of Landsat 5 TM and Landsat 8 OLI, USGS

The calculated radiant temperatures were corrected for emissivity by using the NDVI. The emissivity corrected LST were computed according to [16] and [17] as:

$$LST = \frac{T_B}{1 + \left(\lambda \times \frac{T_B}{p}\right) \ln \varepsilon}$$

Where, T_B is at-satellite brightness temperature (K), w ($\boldsymbol{\lambda}$) indicated wavelength of emitted radiance (wavelength of emitted radiance) (11.5 μm), and P can calculate from the formula of h*c / s (σ) (1.438* 10^{-2} m K). H is Planck's constant (6.626* 10^{-34} J S), S defines the Boltzmann constant (1.38* 10^{-23} J/K), C means velocity of light (2.998* 10^{-8} m/s), the value of P is 14380.

The third phase is the data analysis on the land use/land cover and land surface temperature changes.

The calculated radiant temperatures were corrected for emissivity by using the NDVI. The emissivity corrected LST were computed according to [18] as:

$$LST = \frac{T_B}{1 + \left(\lambda \times \frac{T_B}{p}\right) \ln \varepsilon}$$

Where, T_B is at-satellite brightness temperature (K), w (**λ**) indicated wavelength of emitted radiance (wavelength of emitted radiance) (11.5 μm), and P can calculate from the formula of h*c / s (σ) (1.438* 10^{-2} m K). H is Planck's constant (6.626* 10^{-34} J S), S defines the Boltzmann constant (1.38* 10^{-23} J/K), C means velocity of light (2.998* 10^{-8} m/s), the value of P is 14380.

Results and Discussion

3.1 Spatio-temporal variation of LST and NDVI

LST and NDVI were generated for the years 2006 and 2015 for the Yangon and Mandalay areas as shown in below in Fig. 2. From the visual interpretation of the resulted maps, they were very clear that the area covered by green vegetation contains the lowest temperature and bare land, harvested land and built up areas having the highest temperature of Yangon and Mandalay areas within two study periods.

Table 4 was extracted the mean LST and maximum NDVI value from the classification statistics data. According to this data, although the LST were increased, the maximum value of NDVI were decreased within two study areas. These results showed that the mean LST of Yangon was 33 ºC in 2006 and elevated to 36 ºC in 2015. On the other site, in Mandalay, the mean LST rose from 28.11 ºC in 2006 to 32.43 ºC in 2015.

Table (4). Average LST Changes of Yangon and Mandalay areas (2006-2015) (unit: ºC)

	2006			2015			Change
LST (ºC)	MIN(ºC)	MAX(ºC)	MEAN(ºC)	MIN(ºC)	MAX(ºC)	MEAN(ºC)	MEAN(ºC)
Mandalay	21.17	35.46	28.11	25.18	39.66	32.43	4.32

Source: Image processing of Landsat 5 and Landsat 8 OLI

3.2 Spatio-temporal Changes of LST and NDVI

The information of LST changes in Mandalay area for 2006 and 2015 can be seen at Table 5. These data were calculated the changes of mean temperature 4.3 ºC of Mandalay. The Mean LST of Mandalay area shows 28.11 ºC in 2006 and 32.43 ºC in 2015. The visual situation of vegetation pattern has been found mixed pattern and higher NDVI was covered with the scatter forms and the maximum value lost about 0.03 (0.49 - 0.46) in Mandalay area within the study period.

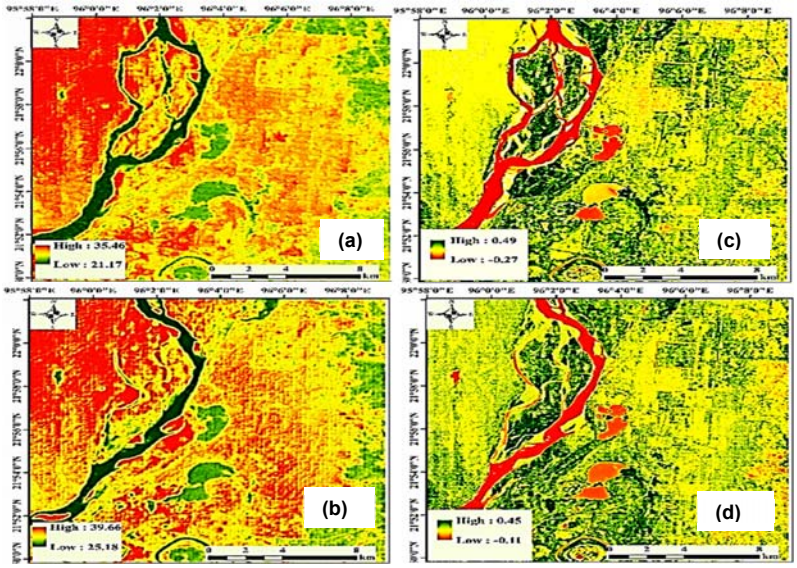

Figure (2). Spatial variation of LST in (a) Mandalay area (2006), (b) Mandalay area (2015),and Spatial variation of NDVI in (c) Mandalay area (2006), (d) Mandalay area (2015)

3.3 Correlating LST and NDVI

Lowest LST was found in areas of high vegetation cover since the amount of vegetation determines the LST by latent heat flux from the atmosphere via evapotranspiration. The correlation between NDVI and LST has shown to be valuable for studies of urban climates. For the LST and NDVI relationship, the values of LST and NDVI of 1556 samples points were selected without water body. In order to disclose the variance of LST and NDVI in different directions, the pixel values of LST and NDVI were derived based on the random samples of two study areas for two periods.

The results were shown by an obvious inverse correlation for both study areas within 2006 and 2015. The association of correlation coefficient of linear regression relationship between LST and NDVI of Mandalay can be seen in Fig. 3. The correlation coefficient result of scatter plot of linear regression was (-0.64) and (-0.7273) of Mandalay for 2006 and 2015.

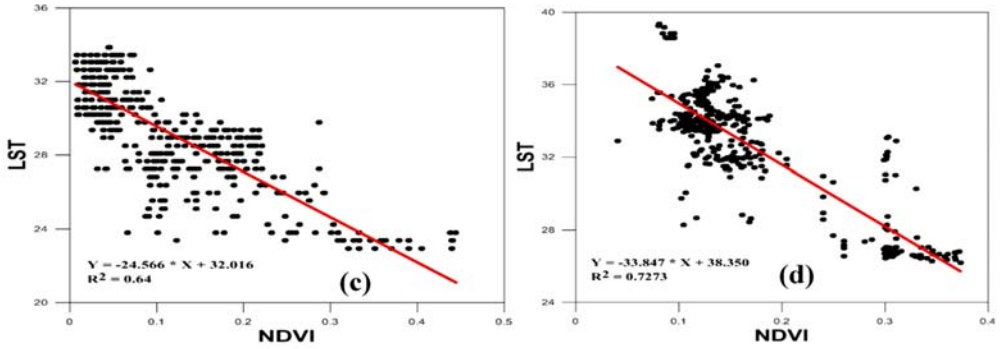

Figure (3). Scatter plot of linear regression analysis between LST and NDVI

Conclusion

(1) **Landsat 5** was a low Earth orbit satellite launched on March 1, 1984 to on June 5, 2013 collect imagery of the surface of Earth. A continuation of the Landsat Program, Landsat 5 was jointly managed by the U.S. Geological Survey (USGS) and the National Aeronautics and Space Administration (NASA). Data from Landsat 5 was collected and distributed from the USGS's Center for Earth Resources Observation and Science (EROS).

(2) **Landsat 8** is an American Earth observation satellite launched on February 11, 2013 to at present. It is also a collaboration between NASA and the United States Geological Survey (USGS). NASA Goddard Space Flight Center in Greenbelt, Maryland, provided development, mission systems engineering, and acquisition of the launch vehicle while the USGS provided for development of the ground systems and will conduct on-going mission operations.

(3) For the LST estimation, different channels are used (band 6 of Landsat 5 and band 10, 11 of Landsat 8). The thermal bands of different channels are different. Moreover, there are several algorithms have been developed to retrieve LST from remotely sensed imageries.

(4) For this study, single channel method is to obtain an algorithm to retrieve LST from the thermal band of the sensor. Main advantage of this algorithm compared with split-window and dual-angle methods that is can be applied to different thermal sensors using the same equation and coefficients.

(5) Mandalay, an inland city, possesses mixed wider vegetation cover and River Ayeyarwady cutting closed with the city have a high influence in moderating the surface temperature.

(6) The study revealed that recorded higher temperature since 2006 to 2015. This was proven by the negative correlations of LST with NDVI. By using multi-temporal remotely sensed data and statistical analysis, this paper was presented better results for the spatiotemporal patterns of LST using fewer remotely sensed data images focusing relatively on Mandalay area.

References

[1] T.W. Owen, T.N. Carlson, and R.R. Gillies, "*An assessment of satellite remotely-sensed land Cover parameters in quantitatively describing the climatic effect of urbanization. International journal of remote sensing*", 1998, Vol. 19, No.9, pp. 1663-1681.

[2] D.R. Streutker, *"Satellite-measured growth of the urban heat island of Houston, Texas. Remote Sensing of Environment",* 2003, Vol. 85, No.3, pp. 282-289.

[3] Q. Weng, and D. Lu, *"A sub-pixel analysis of urbanization effect on land surface temperature and its interplay with impervious surface and vegetation coverage in Indianapolis, United States. International Journal of Applied, Earth Observation and Geoinformation",* 2008, Vol. 10, No.1, pp. 68-83.

[4] E. E. Lambin, H.J.Geist, and E. Lepers, *"Dynamics of Land Use and Cover Change in Tropical Regions. Annual review of environment and resources",* 2003, Vol. 28, No.1, pp. 205-41.

[5] B.L. Turner, *"Local faces, global flowers: the role of land use and land use changes in Datong basin, China, Environmental Geology",* 1994, Vol. 5, No. 2, pp. 1825-1837.

[6] H. Ye, K. Wang, S.Huang, F. Chen, Y. Xiong, and X. Zhao, "*Urbanization effects on summer habitat comfort: A habitat comfort: A case study of three coastal cities in southeast China. International Journal of Sustainable Development and World Ecology"*, 2010, Vol. 17, No.4, pp. 317–323.

[7] Le-Xiang, Hai-Shan, and J.Chang, "*Impacts of land use and cover change on land surface temperature in the Zhujiang Delta. Pedosphere*", 2006, Vol. 16, No.6, pp. 681-689.

[8] W. Kuang, W. Chi, D. Lu, and Y. Dou, *"A comparative analysis of megacity expansions in China and the US: Patterns, rates and driving forces. Landscape and Urban Planning"*, 2014, pp 121-135.

[9] McCarthy, M.J. Best, and R.A. Betts, *"Climate Change in cities due to global warming and urban effects. Geophysical Research Letters"*, 2010, Vol. 37, No. 9, L09705.

[10] M. Jin, R.E. Dickinson, and D.L. Zhang, *"The footprint of urban areas on global climate as characterized by MODIS. Journal of climate"*, 2005, Vol. 18, No.10, pp. 1551-1565.

[11] P.D. Jones, P.Y. Groisman, M. Coughlan, N. Plummer, W. Wang, and T.R. "*Assessment of urbanization effects in time series of surface air temperature over land. Nature*", 1990, Vol. 347, No.6289, pp. 169-172.

[12] C.P. Lo, D.A. Quattrochi, and J.C. Luvall, "*Application of high-resolution thermal infrared remote sensing and GIS to assess the urban heat island effect*". International Journal of Remote Sensing, 1997, Vol. 18, No.2, pp. 287-304.

[13] F. Kraas, H. Gaese, and M.M. Kyi, *Megacity Yangon: Transformation Processes and Modern Developments*, Second German-Myanmar Workshop in Yangon/Myanmar 2005, 2006, Vol. 7. LIT Verlag Münster.

[14] F. Kraas, H.M. Oo, Z.N. Myint, and R. Spohner, *Yangon's Urban Heritage: Reassessing the Historic Stages of Development. Building the Future: The Role of Heritage in the Sustainable Development of Yangon*, 2012, pp. 24-31.

[15] https://en.wikipedia.org/wiki/Mandalay

[16] K.P. Gallo, A.L. McNab, T.R. Karl, J.F. Brown, J.J. Hood, and D.J. Tarpley, The use of a vegetation index for assessment of the urban heat island effect. Remote Sensing, 1993, Vol. 14, No.11, pp. 2223-2230.

[17] R.R. Gillies, and T.N. Carlson, "*Thermal remote sensing of surface soil water content with partial vegetation cover for incorporation into climate models. Journal of Applied Meteorology*", 1995, Vol. 34, No.4, pp. 745-756.

[18] A. Artis, A. David, and W.H. Carnahan, "*Survey of emissivity variability in thermography of urban areas, Remote Sensing of Environment"*, 1982, Vol. 12, No. 4, pp. 313-329.